# Poly(pseudo)rotaxanes formed by mixed micelles and α-cyclodextrin enhance terbinafine nail permeation to deeper layers

Anna Paula Krawczyk-Santos [a], Ricardo Neves Marreto [a], Angel Concheiro [b], Carmen Alvarez-Lorenzo [b,*], Stephânia Fleury Taveira [a,*]

[a] Laboratory of Nanosystems and Drug Delivery Devices (NanoSYS), School of Pharmacy, Universidade Federal de Goiás (UFG), Rua 240, Setor Leste Universitário, 74, 605-170 Goiânia, GO, Brazil
[b] Departamento de Farmacología, Farmacia y Tecnología Farmacéutica, I+DFarma Group (GI-1645), Facultad de Farmacia, iMATUS and Health Research Institute of Santiago de Compostela (IDIS), Universidade de Santiago de Compostela, 15782 Santiago de Compostela, Spain

## ARTICLE INFO

## ABSTRACT

This work aimed to develop water-based formulations for onychomycosis topical treatment using micelles of small pegylated surfactants associated with α-cyclodextrin (αCD) to deliver terbinafine to the nail. Kolliphor® RH40 (RH40) and Gelucire® 48/16 (GEL) single and mixed micelles (RH40:GEL 1:1) were prepared. αCD was added to the surfactants dispersions to form poly(pseudo)rotaxanes (PPR). Formulations were characterized in terms of drug solubilization (3 to 34-fold increase), particle size (9–11 nm) and Z-potential (+0.3 − +1.96 mV), blood compatibility (non-hemolytic), rheological behavior (solid-like viscoelastic properties after 5–10% αCD addition), drug release and interaction with the nail plate. GEL micelles and surfactant-10% αCD PPRs notably hydrated the nail plate. The high viscosity of PPR led to a slower drug release, except for RH40:GEL +10% αCD that surprisingly released terbinafine faster. The RH40:GEL +10% αCD formulation delivered twice more amount of terbinafine to deeper regions of nail plate compared to other formulations. The results evidenced the potential of PPR formed by small pegylated surfactants as a water-based formulation for nail drug delivery.

## 1. Introduction

Onychomycosis, caused by dermatophyte fungi, is the most recurrent disease in the nail plate. Its prevalence worldwide ranges from 2% to 50%, representing about 30% of superficial mycotic infections (Arenas and Torres-Guerrero, 2019). They are cosmetically unpleasant, potentially painful, and challenging to treat (Coleman et al., 2014; Elsayed, 2015; Repka et al., 2002). Oral antifungal therapies are most used for treating onychomycosis; however, they have often been related to important adverse effects. Therefore, topical application is preferable and considered as an unmet clinical need (Arenas and Torres-Guerrero, 2019; Darkes et al., 2003; Uzqueda et al., 2010).

Onychomycosis topical treatment must overcome low nail plate permeability. Nail drug permeation occurs by passive diffusion and is restricted by its highly cross-linked structure, which has disulfide, hydrogen, peptide, and polar bonds (Arenas and Torres-Guerrero, 2019; Baswan et al., 2016; Nair et al., 2009b). Nail formulations should

overcome the restrictions imposed by nail plate structure and adhere to the nail surface, with adequate viscosity to remain at the application site. Currently, solvent-based nail lacquers are available in the market, such as Loceryl® that contains 5% amorolfine and Penlac® or Curanail® that contains 8% ciclopirox (Cutrin-Gomez et al., 2018b). The use of organic solvents in these formulations has significant disadvantages such as irritation and poor drug delivery due to reducing nail hydration and keratin swelling (Cutrin-Gomez et al., 2018b; Gratieri et al., 2017; Vejnovic et al., 2010b). Thus, the obtention of aqueous-based formulations is highly desirable.

Micellar systems may be advantageous for nail delivery because the amphiphilic molecules can interact with water-filled pores in the nail, reducing surface tension, increasing hydration, and nail plate permeability (Chouhan and Saini, 2012). Besides, the combination of amphiphilic molecules and cyclodextrins (CDs) may lead to the formation of poly(pseudo)rotaxanes (PPR) supramolecular gels that can prolong drug permeation at the application site (Lorenzo-Veiga et al., 2019; Marcos
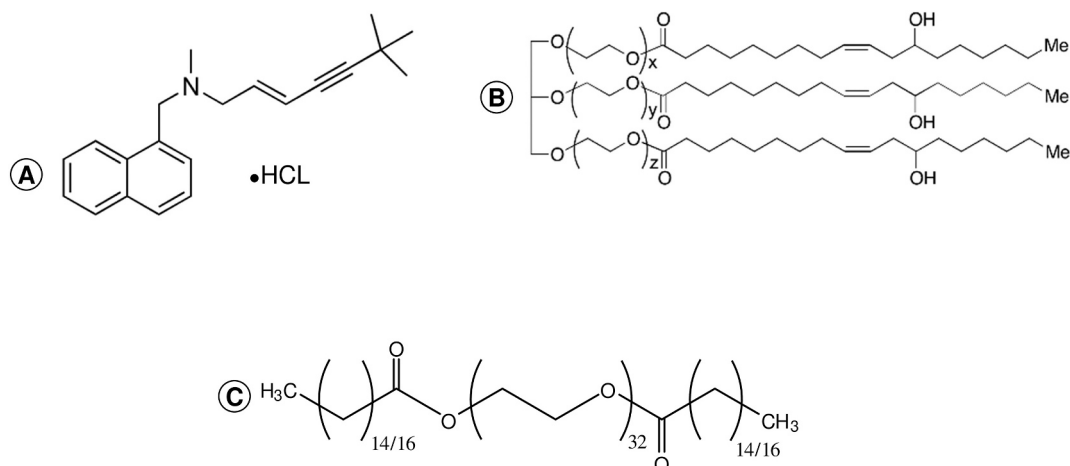
---

**Fig. 1.** Chemical structure of (A) terbinafine hydrochloride (TB) molar mass of 327.17 g/mol, pKa 7.1; (B) Kolliphor® RH40 (RH40) molar mass 2500 g/mol; and (C) Gelucire® 48/16 ($C_{16}$) (GEL) molar mass 1766 g/mol.

et al., 2016; Taveira et al., 2018). These supramolecular gels are viscous systems with a thixotropic behavior suitable for topical application contributing to an adequate spreadability (Marcos et al., 2016; Simões et al., 2015).

PPR proposed for nail delivery have mostly been obtained combining PEG or PEO-based large copolymers and βCD derivatives. For instance, Nogueiras-Nieto et al. (2013) investigated combinations of Pluronic F127 with partially methylated βCD for nail permeation of ciclopirox olamine and triamcinolone acetonide. It was observed that PPR exhibited efficient solubilization properties and remained at the application site. Moreover, the amount of permeated drug was higher compared to a commercial formulation. Subsequently, Cutrin-Gomez et al. (2018a) studied improvements for these systems by obtaining a film-forming and faster drying nail lacquer with good drug permeation. It should be noted that these PPR were hydrosoluble as the βCD mainly threaded along the hydrophobic blocks.

Small pegylated surfactants might also be good candidates for PPR formation, rendering supramolecular structures with αCD and γCD (Taveira et al., 2018). Compared to poloxamers, PEG derivatives with lower molecular weight may be more effective in reducing surface tension (Ogino et al., 1990), and consequently, they can increase nail hydration, favoring drug permeation. Kolliphor® RH40 (PEG-40 hydrogenated castor oil) (RH40) and Gelucire® 48/16 (polyethylene glycol (PEG 32) monostearate) (GEL) (Fig. 1) contain PEG in their composition forming the hydrophilic block. The hydrophobic region comprises castor oil or a mixture of palmitic ($C_{16}$) and stearic ($C_{18}$) acids, respectively. Although these surfactants bear PEG, their ability to form PPR with CDs has not been investigated yet, and their single and mixed micelles have not been explored as nail drug delivery systems. In fact, mixed micelles have gained much attention, as they can take advantage of the sum of performances of each surfactant (Manjappa et al., 2019; Sobczyński and Chudzik-Rząd, 2018).

Terbinafine hydrochloride (TB) (Fig. 1) is the primary drug used for onychomycosis oral treatments. It has excellent fungicide action against dermatophytes (Arenas and Torres-Guerrero, 2019; Uzqueda et al., 2010; Vejnovic et al., 2010a). Despite numerous studies on its topical use (Albarahmieh et al., 2019; Elsherif et al., 2017; Gregori Valdes et al., 2017; Kerai et al., 2018; Patel and Vora, 2016; Tanriverdi et al., 2016; Thatai and Sapra, 2017, 2018), there are still no commercially available topical formulations available.

This work relies on the hypothesis that GEL, RH40 and their combinations can solubilize TB in their micelles and interact with αCD to form PPR that can tune the rheological properties of the dispersions. In addition, micelles or PPR obtained with low molecular weight surfactants may enhance nail hydration and increase TB permeation to deeper nail plate layers. To test these hypotheses, formulations based on single and binary micelles of RH40 and GEL and their combinations with αCD were prepared. The appearance, rheological properties, biocompatibility, nail hydration/porosity, in vitro TB release and hooves permeation were investigated.

## 2. Materials and methods

### 2.1. Materials

Terbinafine hydrochloride (TB) (327.17 g/mol; ≥ 99%) was obtained from Acros Organics™ (New Jersey, USA). Gelucire® 48/16 (1766 g/mol) (GEL) was provided by Gattefossé (Lyon, France), and Kolliphor® RH40 (2500 g/mol) (RH40) was purchased from BASF (Ludwigshafen, Germany). α-Cyclodextrin (αCD) (Cavamax W6 Pharma, lot 60P304, 972.84 Da) was obtained from Wacker Chemie (Munich, Germany). All solvents and reagents were of analytical grade.

Porcine hooves were used as a biological membrane model (Elsayed, 2015). Fresh hooves were obtained at Frigorifico Sol Nascente (Goiânia, Brazil) (CNPJ 73.918.757/0001–31), which local Health Surveillance properly regulates. Hooves were removed from the animal immediately after slaughter and washed with water. Their size and thickness were standardized ($0.25 \pm 0.05$ cm² and $700 \pm 50$ µm, respectively). Hooves were stored at $-20 \pm 2\,°C$ (Naumann et al., 2014; Rocha et al., 2017).

### 2.2. Analytical procedures

TB was quantified by both spectrophotometry and high-performance liquid chromatography (HPLC) with UV detection, and the methods were validated according to the guideline (RDC 166/17) of the Brazilian Health Surveillance Agency (BRASIL, 2017). TB quantification in formulations and release experiments was performed at 283 nm using a UV/Vis spectrophotometer (Thermo 8453, Germany). A linear calibration curve was obtained ($y = 0.0221\times + 0.0127$) in the range from 1 to 40 µg/mL using a mixture of ethanol:water (70:30 $v/v$) as solvent. The method was precise (relative standard deviation for 20 µg/mL was 1.6%) and accurate (expected concentration were $99.40 \pm 2.61\%$, $101.80 \pm 2.05\%$ and $101.28 \pm 2.61\%$ for 1, 20 and 40 µg/mL respectively). The limit of quantitation was 0.45 µg/mL, and the detection limit was 0.15 µg/mL. Selectivity was investigated (formulation components and receptor medium), and no interference was observed at 283 nm.

HPLC method was used for TB quantification in hooves permeation and retention studies. The HPLC system was an Agilent 1260 Infinity II, with a UV detector (G7114A), quaternary pump (G7111B), and auto-

injector system (G7129A) (Agilent Technologies, USA). The mobile phase was comprised of methanol: acetonitrile: water (70:10:20, v/v). The flow rate was 1.2 mL/min, with a detection wavelength of 244 nm. The injection volume was 5 μL. Chromatographic separation was achieved at 60 °C using a C18 column (150 mm; 3 mm, 5 μm) (ZORBAX® Eclipse, Agilent Technologies, USA). The retention time of TB was 4.2 min. A linear calibration curve (y = 980,118× + 60,411, $r^2$ 0.999) was obtained over the concentration range of 1 to 40 μg/mL. The limits of detection and quantitation of the method were 0.04 μg/mL and 0.13 μg/mL, respectively. The method was precise (relative standard deviation for concentration 20 μg/mL was 0.88%) and accurate (expected concentration were 102.68 ± 0.68%, 102.04 ± 0.11% and 101.15 ± 1.04 for 1, 20 and 40 μg/mL respectively). The selectivity was investigated (formulations and hooves homogenates), and no interference was observed in the TB retention time.

### 2.2.1. Drug recovery from hooves membranes

For drug recovery studies, hooves were spiked with a standard TB solution in methanol (80 μg/mL). Then, the solvent was air-dried and the contaminated hooves were submitted to a three-step extraction (Rocha et al. (2017). The steps were as follows: (1) 1 mL of methanol was added to the hooves, followed by magnetic stirring for 2 h (300 rpm, 25 °C). The supernatant was collected for drug quantification ($t = 0$); (2) the same hooves were immersed in 500 μL of fresh methanol for 72 h, the samples were centrifuged, and the supernatant was submitted to a second step of quantification ($t = 72$ h), and (3) the same samples were immersed in 500 μL of fresh methanol for another 72 h (total of 144 h) ($t = 144$ h). TB recovery was the sum of drug content in the three-step extraction procedure (t = 0 + t = 72 h + t = 144 h). TB recovery was 92.69 ± 0.23%.

### 2.3. Solubility studies

#### 2.3.1. Solubility of TB in surfactant dispersions

RH40 and GEL surfactant dispersions (1%, 12%, and 20%, *w/v*) and a mixture of 1:1 RH40 and GEL at 20% (*w/v*) were prepared in test tubes with water or citrate buffer (pH 5.0). TB was then added in excess. All the dispersions were prepared in triplicate and kept under constant stirring for 96 h at 25 ± 2 °C. After that, they were centrifuged at 5000 rpm for 30 min (centrifuge model 5804R, Eppendorf AG, Germany) to separate the non-solubilized drug. Supernatants were diluted in ethanol: water (70: 30, *v/v*) medium, and TB content was determined by UV/Vis spectrophotometry (Thermo 8453, Germany) (see Section 2.2).

The total solubility values of TB in the micellar solution ($S_{tot}$) and in the aqueous media without surfactants ($S_w$) were used to calculate the following parameters (Lorenzo-Veiga et al., 2019; Taveira et al., 2018):

(a) the molar solubilization capacity, X, i.e. moles of drug that can be solubilized per mol of surfactant forming micelles (estimated as the total surfactant concentration, $C_{surfactant}$, minus the critical micelle concentration, CMC):

$$X = \frac{S_{tot} - S_w}{C_{surfactant} - CMC} \quad (1)$$

(b) the micelle-water partition coefficient (ratio between the drug concentration in micelle and the aqueous phase):

$$P = \frac{S_{tot} - S_w}{S_w} \quad (2)$$

(c) the molar micelle-water partition coefficient (*PM*) for a default concentration of 1 M surfactant:

$$PM = \frac{X \cdot (1 - CMC)}{S_w} \quad (3)$$

(d) the Gibbs standard-free energy of solubilization (*R* being the universal constant of gases):

$$\Delta G_s = -RT \cdot \ln(PM) \quad (4)$$

(e) the proportion of drug molecules encapsulated in the micelles (*mf*):

$$mf = \frac{S_{tot} - S_w}{S_{tot}} \quad (5)$$

#### 2.3.2. Solubility of TB in surfactant dispersions with αCD

RH40, GEL, and 1: 1 mixed dispersions (RH40:GEL) were prepared in citrate buffer (pH 5.0) and placed in test tubes. TB was added and, after 24 h of magnetic stirring, αCD was added up to a final concentration of 1%, 5%, and 10% (*w/v*). The dispersions were kept under magnetic stirring for 96 h and then were centrifuged at 5000 rpm for 30 min. Supernatants were diluted in ethanol: water (70: 30, *v/v*) mixture for TB quantification (see Section 2.2). TB solubility in αCD solutions (1%, 5%, and 10%, w/v) was also investigated.

### 2.4. Micelles preparation and characterization

RH40, GEL and RH40:GEL mixed micelles (1%, 12%, and 20%, w/v) were prepared by dispersing the surfactants in water or citrate buffer (pH 5.0), under constant stirring. The pH of dispersions was recorded. The mean diameter, polydispersity index (PdI), and zeta potential of the formed micelles were determined using a Zetasizer Nano ZS (Malvern Instruments, UK). TB-loaded micelles (2%, *w/w*) were obtained by adding TB to the surfactant dispersion which was kept under stirring for 24 h and afterward characterized.

### 2.5. Preparation of poly(pseudo)rotaxanes (PPR)

RH40, GEL, and RH40:GEL dispersions (20%, w/v) were prepared in citrate buffer (pH 5.0). 2% (w/v) of TB was added, and systems were kept under magnetic stirring for 24 h at room temperature. Next, αCD was added (1, 5, and 10%) to each dispersion and homogenized for 10 min for PPR formation. The formulations were prepared stored at 4.0 ± 0.0 °C before use.

### 2.6. Gel appearance and microstructure

Changes in turbidity were examined by visual inspection, and gel formation was monitored by applying an inverted tube test. Pictures were taken to compare the visual changes of different surfactant dispersions.

Transmission Electronic Microscopy (TEM) images of micelles and PPR systems were recorded using a Jeol microscope (JEM 2100 Tokyo, Japan) equipped with EDS (Thermo Scientific, Japan) at the High-Resolution Microscopy Laboratory of the Federal University of Goiás (LabMic, UFG). The samples were diluted in distilled water (1:5 for micelles and 1:100 for PPR). A drop of each was applied to copper grids and maintained for 10 min. The sample excess was removed, and uranyl acetate was placed over the dry samples and kept for 3 min, followed by drying at room temperature and analysis under a microscope at a voltage of 200 kV.

### 2.7. Rheological characterization

Storage (G') and loss (G") moduli of RH40 (20%), GEL (20%), RH40: GEL (20%) (1:1) and PPR formed from these dispersions in citrate buffer were recorded in a Rheolyst AR-1000 N rheometer (TA Instruments, New Castle, DE, USA) equipped with an AR2500 data analyzer, a Peltier plate, and cone geometry (6 cm diameter, 2.1°). Studies were performed at a fixed angular frequency of 5 rad/s and a temperature ramp of 1 °C/min from 20 to 35 °C.
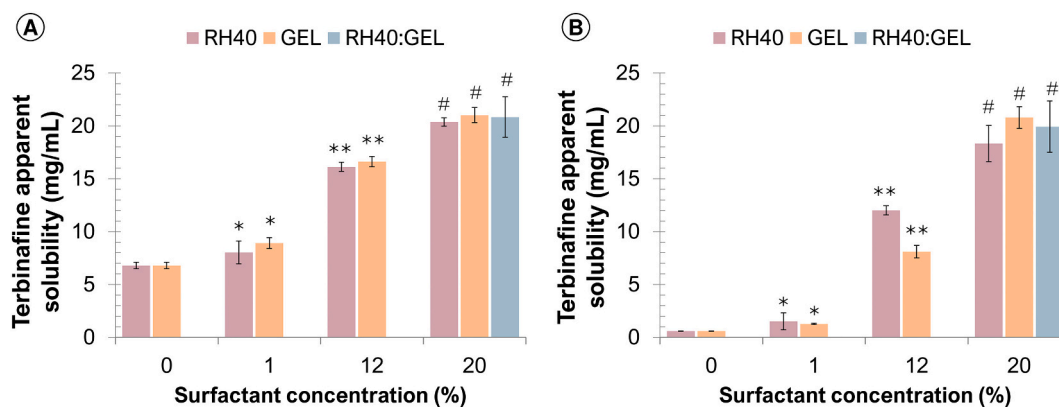
**Fig. 2.** Apparent solubility of TB in RH40, GEL and mixed formulations (RH40:GEL) in: a) water and b) citrate buffer (pH 5.0). *,#Symbols indicate statistically significant differences ($p < 0.05$).

### 2.8. Hemolysis assay

The capacity of formulations to trigger a hemolytic event was tested. 20% ($w/v$) micelles with and without 5% αCD were diluted with 0.9% NaCl aqueous solution (1:10), resulting in concentrations of 2% RH40, GEL and RH40:GEL and 0.5% αCD. Fresh blood was obtained from Galician Transfusion Center (Spain) from anonymous volunteers and diluted (1:30) with 0.9% NaCl aqueous solution. Aliquots of diluted blood (900 μL) were added to the diluted formulation samples (100 μL). The mixture was incubated for 60 min at 37 °C in a mini shaker at 100 rpm. The release of hemoglobin was determined after centrifugation (10,000 rpm for 10 min) by recording the supernatant absorbance at 542 nm in a plate reader (Fluostar Optima, BMG Labtech, Germany). The negative and positive controls were 0.9% NaCl solution and 4% ($v/v$) Triton X-100, respectively. Hemolysis was calculated as follows:

$$Hemolysis \ (\%) = \frac{(A_S - A_N)}{(A_P - A_N)} \times 100 \qquad (6)$$

In this equation, $A_S$ represents the sample absorption value, $A_N$ the negative control absorption value, and $A_P$ the positive control absorption value.

### 2.9. Hooves hydration and microstructure after immersion in different formulations

#### 2.9.1. Hydration study

First, hooves had their size and thickness adjusted with the aid of a scalpel and a digital caliper (Mitutoyo, São Paulo, Brazil) to be 0.25 ± 0.05 cm$^2$ and 700 ± 50 μm, respectively. Then, they were oven-dried overnight at 45 ± 0.5 °C. For the hydration study, hooves were weighed and placed in vials filled with 1 mL of each developed formulation ($n = 3$). The vials were sealed and kept at 25 ± 2 °C for 24 h. Control samples were obtained by immersing hooves in 1 mL of citrate buffer (pH 5.0). After 24 h, hooves were withdrawn from the vials and wiped with tissue paper to remove any residue of formulation from their surface. Samples were weighed again, and the hydration enhancement factor (HEF24) for each formulation was calculated as the ratio of the weight gain of hooves exposed to formulations (*Wp*) compared to the weight gain of hooves exposed to control (*Wc*) (Chouhan and Saini, 2012; Krawczyk-Santos et al., 2021; Rocha et al., 2017), according to Eq. (7).

$$HEF24 = \frac{Wp}{Wc} \qquad (7)$$

#### 2.9.2. Hooves microstructure study by scanning electron microscopy (SEM)

SEM images were taken from the hooves surface before and after immersion in each developed formulation for 24 h. Hooves were coated with gold using Denton Vacuum sputter coater (Desk V, Moorestown, EUA). SEM images were taken from hooves surface using a Jeol microscope (JSM 6610, Tokyo, Japan) equipped with an X-ray detector by energy dispersive spectrometry (Thermo Scientific NSS) with a spectral imaging system (Thermo Scientific, Madison, USA). The analysis was performed at the High-resolution Microscopy Laboratory of the Federal University of Goiás (LabMic).

### 2.10. Release studies

TB in vitro release was evaluated using a Franz-type diffusion cell and cellulose acetate dialysis membrane (MWCO 12,000-14,000, Sigma Aldrich, Germany). The receptor medium was distilled water (6 mL). 500 μL of all developed formulations (micelles and PPR) containing 2% TB ($w/v$) were placed in the donor compartment. The total amount of drug in the donor compartment was 10 mg, and the area available for diffusion was 0.785 cm$^2$. The stirring rate and temperature of the receptor chamber were kept at 650 rpm and 32 ± 0.5 °C, respectively. Each experiment was performed for 24 h and under sink conditions. At appropriate intervals (1, 2, 4, 6, 10, and 24 h), aliquots of the receptor media (1 mL) were withdrawn and immediately replaced with equal volumes of fresh receptor media. The amount released was determined by UV/Vis spectrophotometry.

Flux ($J$) was calculated as the slope ($Q / t$) of the linear section of the amount of drug released in the receptor chamber ($Q$) versus time ($t$). Each experiment was performed in triplicate.

### 2.11. In vitro permeation studies

Permeation studies were also performed in vertical diffusion cells in which hooves were mounted using nail adapters (PermeGearm Inc., USA). The ventral part was placed facing downward into the receptor media (distilled water). The donor chamber was then filled with 500 μL of each micellar and PPR formulations containing 2% (w/v) of TB. Experiments were performed under sink conditions ($n = 4$) with a stirring rate of 650 rpm and 32 °C.

After permeation, hooves were removed, and the excess of the formulation was removed with a paper towel. Hooves were then sliced using a scalpel. The splinters were transferred to a glass vial, and the extraction procedure was performed as described in Section 2.2.

### 2.12. Statistical analysis

GraphPad Prism version 8.2.1 (441) (Graphpad Prism inc., USA) was used for statistical analysis. The statistical significance of experiments was determined using *t*-test nonparametric or ANOVA followed by Tuckey. Tests yielding *p* values <0.05 were considered significant.

**Table 1**
Parameters that characterize the ability of GEL and RH40 micelles to solubilize TB in water and citrate buffer (estimated using Eqs.1–4).

| Water pH 5.7 | | | | | | | | |
|---|---|---|---|---|---|---|---|---|
| RH40 (%, w/v) | RH40 (M) | TB (mg/mL) | TB (M) | X | P | PM | ΔGs (KJ/mol) | mf |
| 1 | 0.0040 | 8.03 | 0.0245 | 0.96 | 0.18 | 46.42 | −9503.83 | 0.15 |
| 12 | 0.0480 | 16.12 | 0.0493 | 0.59 | 1.37 | 28.65 | −8308.47 | 0.58 |
| 20 | 0.0800 | 20.37 | 0.0623 | 0.52 | 2.00 | 25.01 | −7971.86 | 0.67 |
| GEL (%, w/v) | GEL (M) | TB (mg/mL) | TB (M) | X | P | PM | ΔGs (KJ/mol) | mf |
| 1 | 0.0057 | 8.91 | 0.0272 | 1.14 | 0.31 | 55.07 | −9926.87 | 0.24 |
| 12 | 0.0680 | 16.62 | 0.0508 | 0.44 | 1.45 | 21.29 | −7572.85 | 0.59 |
| 20 | 0.1133 | 21.01 | 0.0642 | 0.38 | 2.09 | 18.49 | −7223.75 | 0.68 |
| RH40:GEL 1:1 (%, w/v) | | TB (mg/mL) | | | P | | | mf |
| 20 | | 20.83 | | | 2.07 | | | 0.67 |
| | | | | | | | | |
| Citrate Buffer pH 5.0 | | | | | | | | |
| RH40 (%, w/v) | RH40 (M) | TB (mg/mL) | TB (M) | X | P | PM | ΔGs (KJ/mol) | mf |
| 1 | 0.0040 | 1.51 | 0.0046 | 0.72 | 1.57 | 401.06 | −14,843.70 | 0.61 |
| 12 | 0.0480 | 12.01 | 0.0367 | 0.73 | 19.47 | 406.32 | −14,876.96 | 0.95 |
| 20 | 0.0800 | 18.33 | 0.0560 | 0.68 | 30.24 | 378.36 | −14,699.41 | 0.97 |
| GEL (%, w/v) | GEL (M) | TB (mg/mL) | TB (M) | X | P | PM | ΔGs (KJ/mol) | mf |
| 1 | 0.0057 | 1.27 | 0.0039 | 0.37 | 1.17 | 206.17 | −13,195.87 | 0.54 |
| 12 | 0.0680 | 8.11 | 0.0248 | 0.34 | 12.82 | 188.66 | −12,976.03 | 0.93 |
| 20 | 0.1133 | 19.34 | 0.0591 | 0.51 | 31.97 | 282.26 | −13,973.77 | 0.97 |
| RH40:GEL 1:1 (%, w/v) | | TB (mg/mL) | | | P | | | mf |
| 20 | | 19.92 | | | 32.96 | | | 0.97 |

X: molar solubilization capacity; P: partition coefficient; PM: molar partition coefficient; mf: molar fraction of drug encapsulated in the micelle.

Results were reported as mean values ± standard deviation (SD).

## 3. Results and discussion

### 3.1. TB solubilization in GEL, RH40 and mixed dispersions

TB solubility in water was 6.79 ± 0.30 mg/mL (Fig. 2), which agrees with previous studies (Chouhan and Saini, 2014; Lusiana and Muller-Goymann, 2011). At water pH (slightly acid), TB is ionized and has good solubility (Sachdeva et al., 2010; Uzqueda et al., 2009). However, TB solubility in citrate buffer (pH 5.0) was significantly lower, i.e., 0.59 ± 0.01 mg/mL ($p < 0.05$), probably due to a salting out effect caused by the ionic strength of the buffer.

TB solubility increased as the surfactant concentration increased, even at the lowest concentration tested (Fig. 2). Surfactant concentrations were above the CMC, i.e., 0.020% and 0.015% for RH40 and GEL, respectively (BASF, 2011; Gattéfossé, 2018), which enabled TB solubilization into the micelles. Both surfactants showed similar behavior, and almost no differences in solubilization capacity were observed for a given concentration and media (Fig. 2). RH40 and GEL 20% (w/v) dispersions solubilized 2% (w/v) of TB. This TB concentration was in the 1 to 10% range chosen in previous attempts of development of ungual formulations for onychomycosis treatment (Ghannoum et al., 2019; Ghannoum et al., 2009; Nair et al., 2009a; Shivakumar et al., 2010; Thatai and Sapra, 2017, 2018).

Parameters used to quantify the efficiency of solubilization are summarized in Table 1. The micelle-water partition coefficient (P) was higher for micelles in the buffer, which means that the less favorable medium provided by citrate buffer enhanced TB interaction with the micelle inner core. These results were also supported by the higher proportion of drug encapsulated in micelles (mf) in buffer medium, reaching values close to 100% of drug molecules encapsulated.

ΔGs was negative in all cases indicating that the solubilization occurred spontaneously, probably due to the hydrophobicity of the micelle core, as also reported for macrogol micelles (Zhou et al., 2017). The molar solubilization capacity (X) decreased with the increase of surfactant concentration (Table 1), which suggests that as surfactant concentration increases the micelles are formed by more unimers (Lorenzo-Veiga et al., 2019). However, GEL 20% in buffer media behaved differently and showed increasing molar solubilization capacity (X)
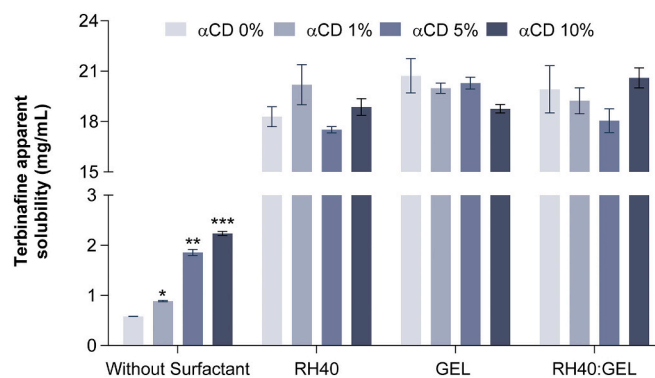


**Fig. 3.** Apparent solubility of TB in formulations prepared with 0, 1, 5 and 10% of αCD with and without 20% (w/v) of RH40, GEL and RH40:GEL in citrate buffer pH 5.0 ($n = 3$). *Symbols indicate statistically significant differences ($p < 0.05$).

values, probably due to a different organization of this surfactant in buffer media.

The RH40:GEL 1:1 mixed micelles solubilized 20.83 ± 1.92 mg/mL and 19.92 ± 2.44 mg/mL of TB in water and in buffer medium, respectively. Also, the partition coefficient (P) was higher in buffer than in water (32.96 and 2.07, respectively) as well as the proportion of drug molecules encapsulated in the micelles (0.97 and 0.67, respectively). According to their high solubilizing capacity, micelles prepared with single and mixed surfactants at 20% were selected for subsequent studies.

### 3.2. TB solubility in surfactant dispersions with αCD

TB solubility was investigated in αCD dispersions and surfactant dispersions (20%, w/v) combined with αCD (Fig. 3) in citrate buffer pH 5.0. The increase of αCD concentration in formulations without surfactants resulted in a linear enhance in drug solubility. For instance, 10% of αCD increased about 3.8-fold TB solubility. Nevertheless, this increase was relatively lower than for the formulations that combined surfactants and αCD ($p < 0.05$). The lower solubilization capacity of αCD dispersions, compared to the micelles, may be related to the small size of the

**Table 2**

Micelle diameter (nm) in volume-based distribution, polydispersity index (PdI) and zeta potential of RH40, GEL and RH40:GEL 1:1 mixed formulation prepared with 20% of surfactants (w/w) dispersed in citrate buffer (pH 5.0) and loaded or not with 2% (w/v) of TB (n $\geq$ 3).

| Formulations 20% (w/v) | Mean diameter (nm) | | PdI | | Z-Potential (mV) | |
|---|---|---|---|---|---|---|
| | Unloaded | Loaded | Unloaded | Loaded | Unloaded | Loaded |
| RH40 | 10.61 ± 0.78 | 10.18 ± 0.16 | 0.064 ± 0.02 | 0.110 ± 0.01 | 0.78 ± 0.37 | 1.24 ± 0.63** |
| GEL | 9.17 ± 0.66 | 9.78 ± 0.11 | 0.673 ± 0.17* | 0.594 ± 0.40* | 0.30 ± 0.13 | 1.59 ± 0.35** |
| RH40:GEL (1:1) | 9.43 ± 0.96 | 10.24 ± 0.18 | 0.538 ± 0.04* | 0.466 ± 0.10* | 0.68 ± 0.39 | 1.96 ± 0.83** |

* Higher PdI for GEL and RH40: GEL 1:1 compared to RH40.
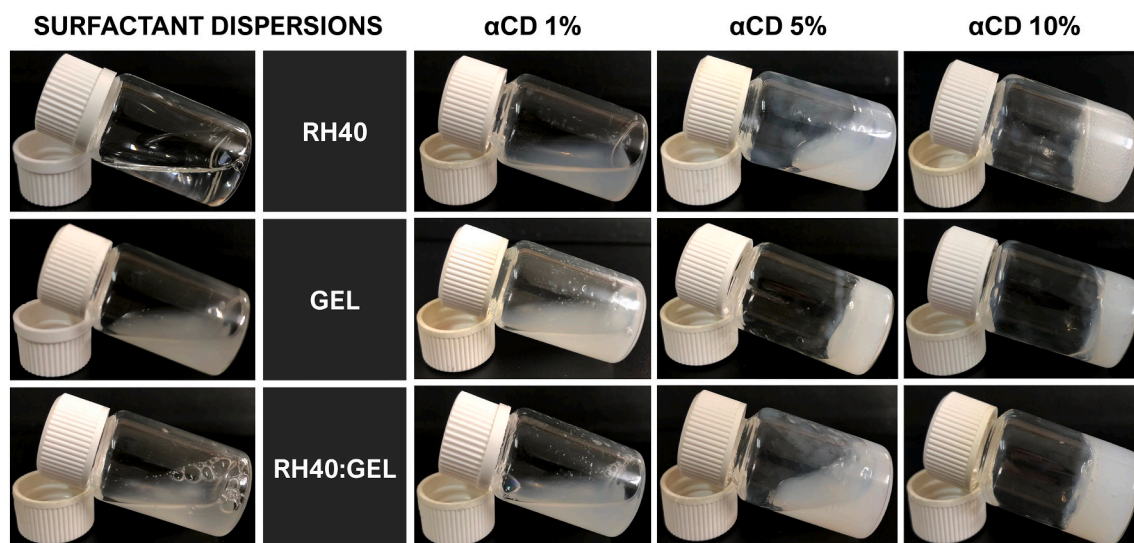** Higher zeta potential for loaded micelles.



**Fig. 4.** Pictures of surfactant dispersions (20%, w/v) combined with 1, 5, or 10% of αCD in citrate buffer (pH 5.0). PPR formation was observed immediately after preparation.

αCD cavity, which does not allow for a complete inclusion of the TB naphthalene ring. The complexation of TB with αCD could be related to weak interactions of TB aliphatic chain in the cavity of αCD (Uzqueda et al., 2009).

All surfactant-αCD systems showed similar TB solubilization capability, disregarding the content in αCD ($p > 0.05$) (Fig. 3) and the order of addition of drug and αCD (data not shown). In all cases the formulations were kept under stirring for 24 h before characterization, and this time may be sufficient for the ternary system to reach the equilibrium disregarding the order of addition. Some authors reported that PPR formation can be detrimental to drug solubilization (Szente et al., 2014). RH40 and GEL have free low molecular weight PEG in their composition, and thus αCD units might be threading these free PEG chains to form PPR, not disturbing the micellar core structure, which remains available for solubilizing the drug (Taveira et al., 2018). Besides, αCD could also interact with PEG chains at the micelles corona, causing minor changes in their conformation. PPR formation was further investigated in next sections (Sections 3.4 and 3.5).

### 3.3. Micelles characterization

Size and Z-potential of RH40 and GEL dispersions in water (Table S1 – Supplementary material) and citrate buffer (Table 2) were measured. Water dispersions showed a variety of pH values, and for GEL the pH decreased from 5.27 to 3.89 as the concentration increased from 1 to 20%. These dispersions also resulted in a lower molar fraction of drug encapsulated in the micelles (Table 1). This problem was overcome with the use of citrate buffer pH 5.0 which revealed to be a good dispersant for RH40, GEL, and their mixture, also enabling excellent drug encapsulation (Table 1).

The relatively low molecular weight of the surfactants (2500 g/mol for RH40 and 1766 g/mol for GEL) resulted in small micelles (~10 nm). RH40 micelles consisted in a monodisperse size distribution with a low PdI value of 0.065 (Table 2). Differently, GEL dispersion were polydisperse in size with PdI values of 0.673. These surfactants are obtained from an esterification process between PEG and lipids, i.e., GEL is obtained with stearic and palmitic acid, and RH40 with castor oil. The reaction products result in a mixture of compounds that vary in chain lengths (Casiraghi et al., 2015; Hussein and Youssry, 2018). Comparison of DLS results in terms of intensity and volume revealed that GEL dispersions contained larger aggregates in coexistence with small micelles (Fig. S1 - Supplementary material). The RH40:GEL 1:1 mixture led to micelles with mean diameter and polydispersity close to those of GEL solely micelles.

The addition of TB to the micelles did not cause significant changes in the size of micelles dispersed in citrate buffer (Table 2), but slightly increased zeta potential values ($p < 0.05$) (Table 2), probably due TB ionization (pKa 7.1) (AbdelSamie et al., 2016).

### 3.4. PPR formation and gels appearance

The addition of αCD to the micellar dispersions caused that the initial translucid (RH40) or opalescent (GEL and RH40:GEL) dispersions turned into whitish systems (Fig. 4) with increased viscosity when αCD was added at 5 and 10%. No visual changes in viscosity were observed with the addition of 1% αCD. This is the first time RH40 and GEL have been used together with αCD to form these systems. The whitish color was a clear indication of PPR formation (Marreto et al., 2020; Taveira et al., 2018).

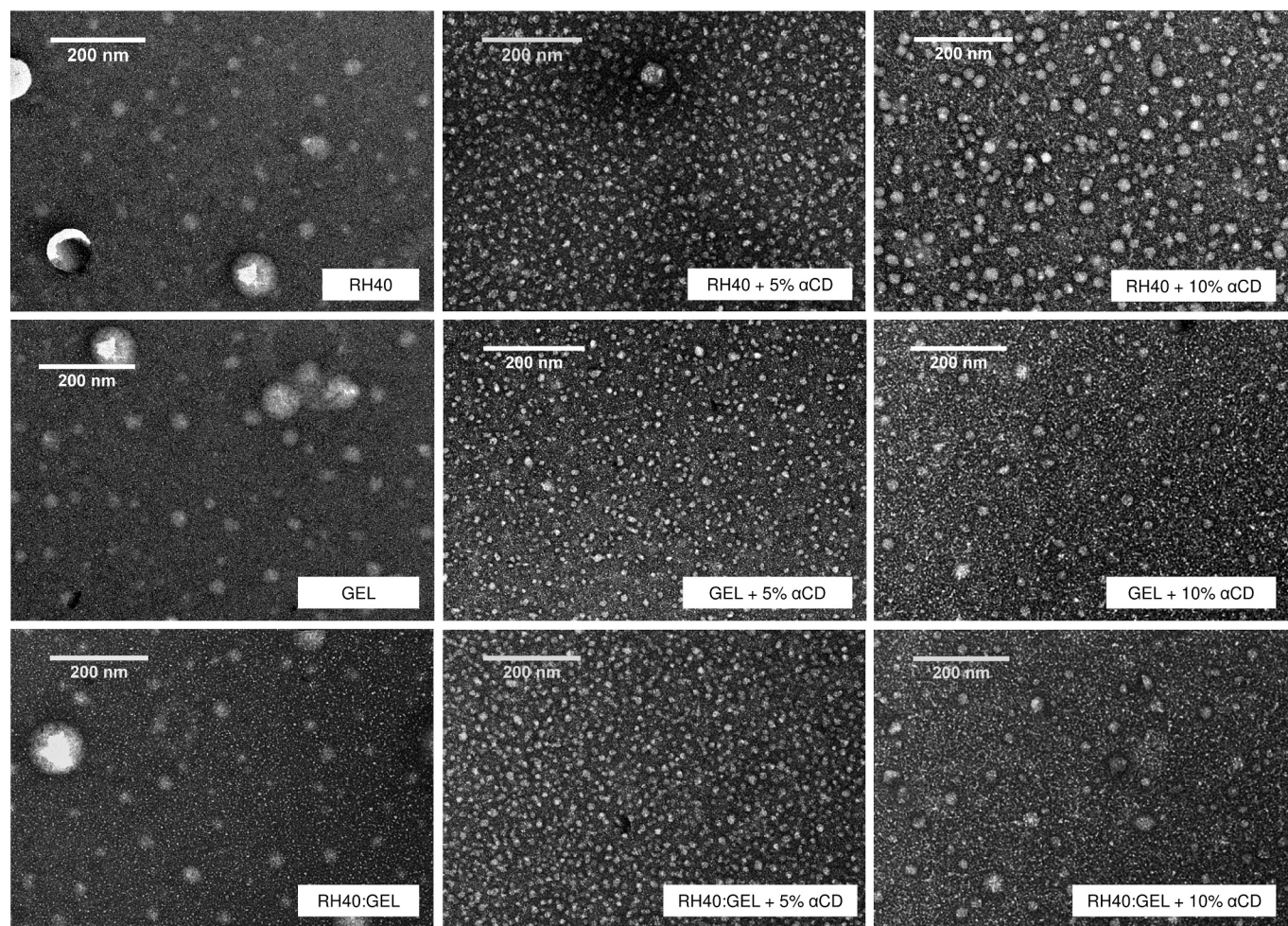TEM images of RH40, GEL, and RH40:GEL dispersions confirmed the

**Fig. 5.** TEM images of RH40, GEL and RH40:GEL dispersions (20%, w/v) with and without αCD at 5 and 10%.

formation of spherical micelles (Fig. 5) with diameters that agreed well with the DLS results. Formulations with αCD (PPR) showed significantly different images. Despite they were diluted, the background of TEM images was more irregular than in the case of the micelles (Fig. 5). The appearance of numerous structures, with more elongated shape, probably came from the interaction between the surfactants and αCD leading to PPR. The addition of αCD at 10% resulted in some larger structures than those observed in the presence of αCD at 5%.

### 3.5. Rheological properties

The viscoelastic behavior of surfactant dispersions with and without αCD was determined to assess PPR formation and its dependence on temperature (Fig. 6). In the absence of αCD, RH40 dispersion showed temperature dependence and performed as a liquid-like material at 20 °C, with negligible storage modulus (G'). The temperature rise led to a sol-to-gel transition at 34 °C. G' values became evident and larger than G", with an increase of about three orders of magnitude (Fig. 6A). Differently, GEL dispersion did not present a temperature-dependent behavior, and G" values were almost two-orders of magnitude above those of RH40 dispersion at room temperature. GEL dispersions also exhibited noticeable G' values in the temperature range evaluated, although below G" values, performing as liquid-like systems. The mixture of surfactants (RH40:GEL 1:1) showed G" values in between those of each dispersion in separate with a slight dependence on temperature as a result of RH40 influence. There was a gentle increase in G" at 30 °C, and G' became evident with the rise in temperature at 32 °C.

However, no sol-gel transition occurred below 35 °C (Fig. 6A). Thus, differently to the most tested amphiphilic block copolymers based on poloxamers or Soluplus (Lorenzo-Veiga et al., 2019; Nogueiras-Nieto et al., 2013), the use of RH40 and GEL has the advantage of allowing to reach quite high surfactant (and thus micelles) concentrations without an excessive increase in viscosity, which may facilitate both drug loading into the micelles and the subsequent spreadability of the formulation on the nail.

The addition of 1% αCD to the surfactant dispersions did not cause notable changes in rheological behavior (G" values remained similar) but G' values (still small) were recordable in the whole range of temperature (Fig. 6B, C, and D), which suggests some structuring of the surfactant assemblies. Differently, higher concentrations of αCD (5 and 10%) made G' to become larger than G", indicating the formation of three-dimensional networks, typical of PPR supramolecular interactions. The moduli of GEL PPR were larger than those of RH40 and RH40:GEL. The temperature dependence of RH40 also influenced PPR behavior. When 5% αCD was added to the surfactant dispersion, and the temperature was raised at 26 °C, the moduli progressively increased (approx. One order of magnitude). The temperature effect was not observed when 10% αCD was added, probably because the supramolecular complexes formed in the presence of such a high αCD concentration and the subsequent 3D stacking of the PPR through semi-crystalline interactions among the threaded αCDs provided a highly viscoelastic network at room temperature (Taveira et al., 2018). PPR obtained from mixed dispersions presented an intermediary G' and G" values. Temperature slightly affected the moduli and only a gentle
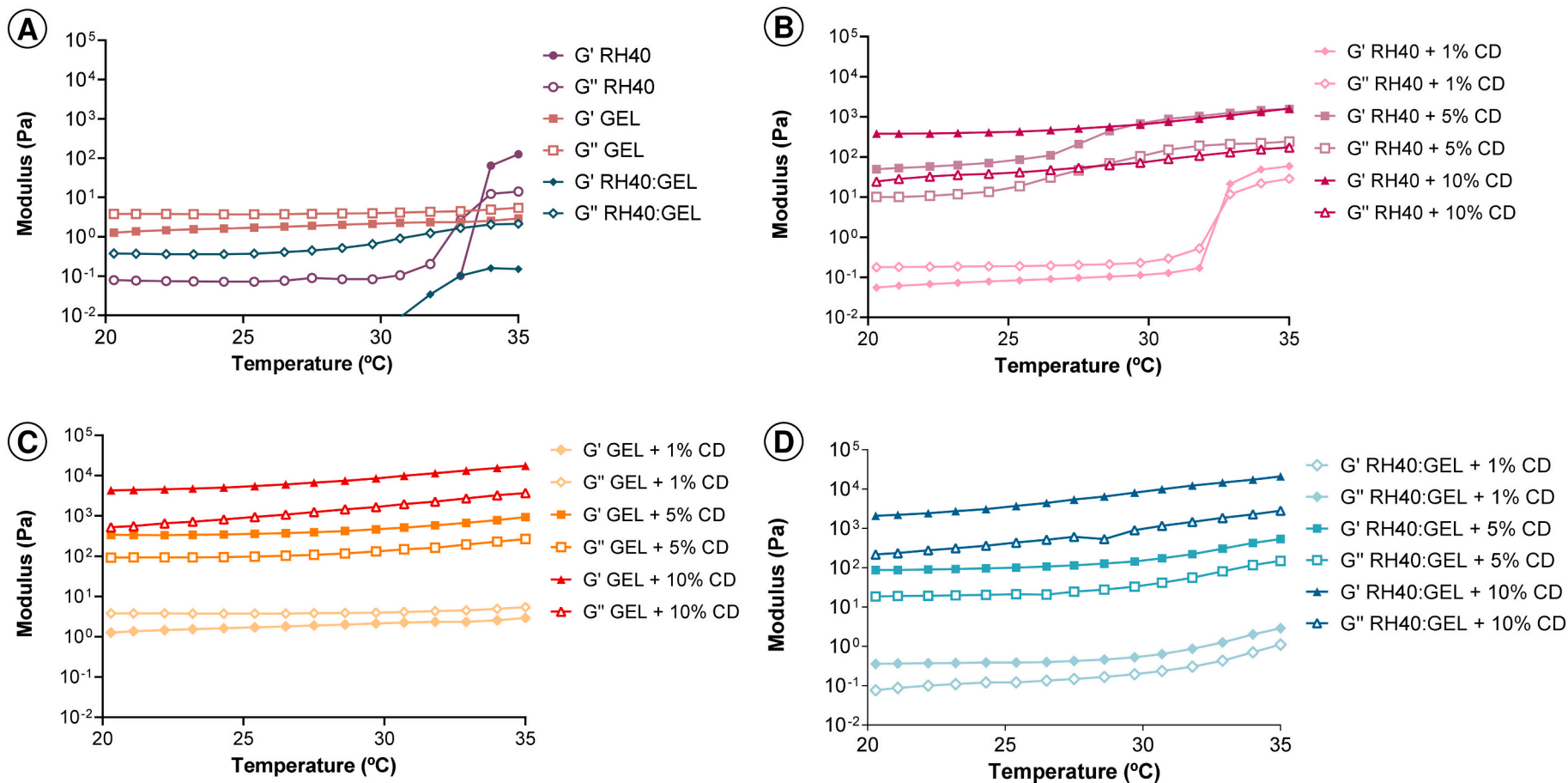
**Fig. 6.** Evolution of the storage (G') and loss (G'') moduli as a function of temperature: a) surfactant dispersions, b) RH40 with αCD, c) GEL with αCD, and d) RH40: GEL (1:1) with αCD.
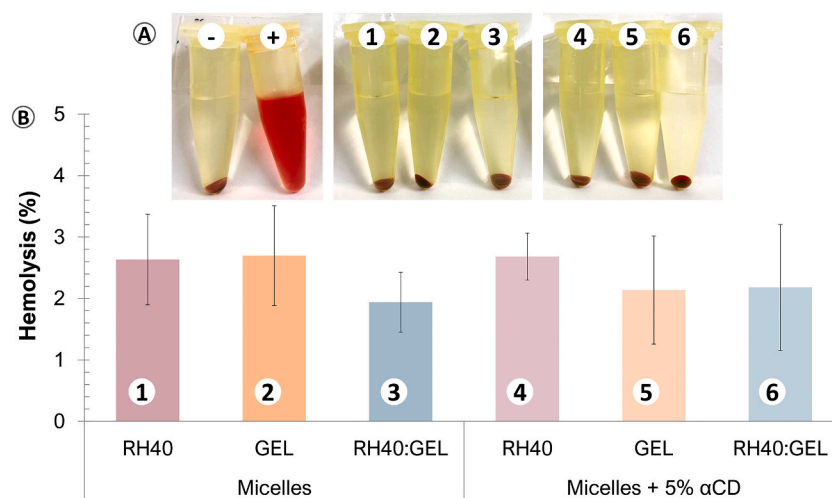
**Fig. 7.** Picture (A) and percentage (B) of hemolysis produced by formulations after 1 h of incubation. 0.9% NaCl and 4% Triton X-100 aqueous solution were used as negative (−) control (0% hemolysis) and positive (+) control (100% hemolysis), respectively. Formulations were diluted 1:10 in 0.9% NaCl. 1) RH40, 2) GEL, 3) RH40:GEL, 4) RH40 + 5% αCD, 5) GEL +5% αCD and 6) RH40:GEL +5% αCD.
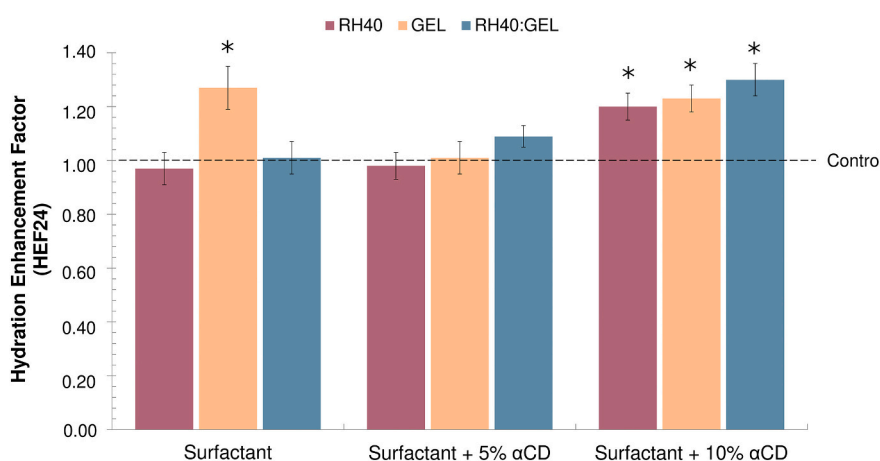


**Fig. 8.** Hydration enhancement factor (HEF24) of hooves treated with the GEL, RH40, GEL: RH40 (1:1) without CD and formulations with 5 and 10% of αCD. *Symbols indicate statistically significant differences (p < 0.05).

increase was observed when αCD 5% was added (Fig. 6D). In the case of systems containing αCD 10%, G′ and G″ values were in between those of the PPR obtained with each surfactant in separate.

In sum, the addition of αCD increased the viscosity of the formulation through PPR formation. Supramolecular gels formed with 10% αCD seem to be the most promising due to their higher viscosity under low stress conditions (i.e., at rest), which could prevent the formulation from leaking when topically applied.

### 3.6. Hemolysis assay

The hemolysis assay can inform about the biocompatibility of materials used in drug formulation (Amin and Dannenfelser, 2006). It should be taken into account that 10% αCD solutions directly added to erythrocytes may cause strong hemolysis (Motoyama et al., 2006). Nevertheless, αCD has been shown to be safe for ocular application at concentrations up to 4% (EMA, European Medicines Agency, 2014). Micelles and PPR formulations were diluted, considering that the formulation components would hardly be absorbed in the concentrations used for its production. Even at concentrations greater than 2% surfactants and 0.5% αCD, no hemolysis was recorded (Fig. 7), and no statistical difference was observed compared to the negative control (p > 0.05). According to ISO 10993-part 4 (2017) hemolysis values lower than 5% mean that the formulation is non-hemolytic.

### 3.7. Hooves hydration and microstructure: The influence of micelles and PPR formulations

#### 3.7.1. Hydration study

Drug diffusion through the nail plate is closely related to the thickness and hydration of the membrane. When the nail plate absorbs water, pores can increase in number and size, an expansion of the structure occurs, increasing the porosity of the previously compact internal area. Hydrated nails also become more elastic, facilitating the permeation of different molecules (Chouhan and Saini, 2012; Cutrin-Gomez et al., 2018c; Gunt et al., 2007; Krawczyk-Santos et al., 2021; Nogueiras-Nieto et al., 2011). The effects of the formulations on the nail plate were quantified by means of the hydration enhancement factor (HEF24) (Fig. 8).

GEL micelles were the ones that best hydrated the hooves when compared to RH40, mixed micelles, and the control (p < 0.05). The PEG units present in the surfactants can positively influence nail hydration by improving the interaction of water molecules with the polar groups in keratin, which results in greater water absorption and swelling of the structure (Nair et al., 2010).

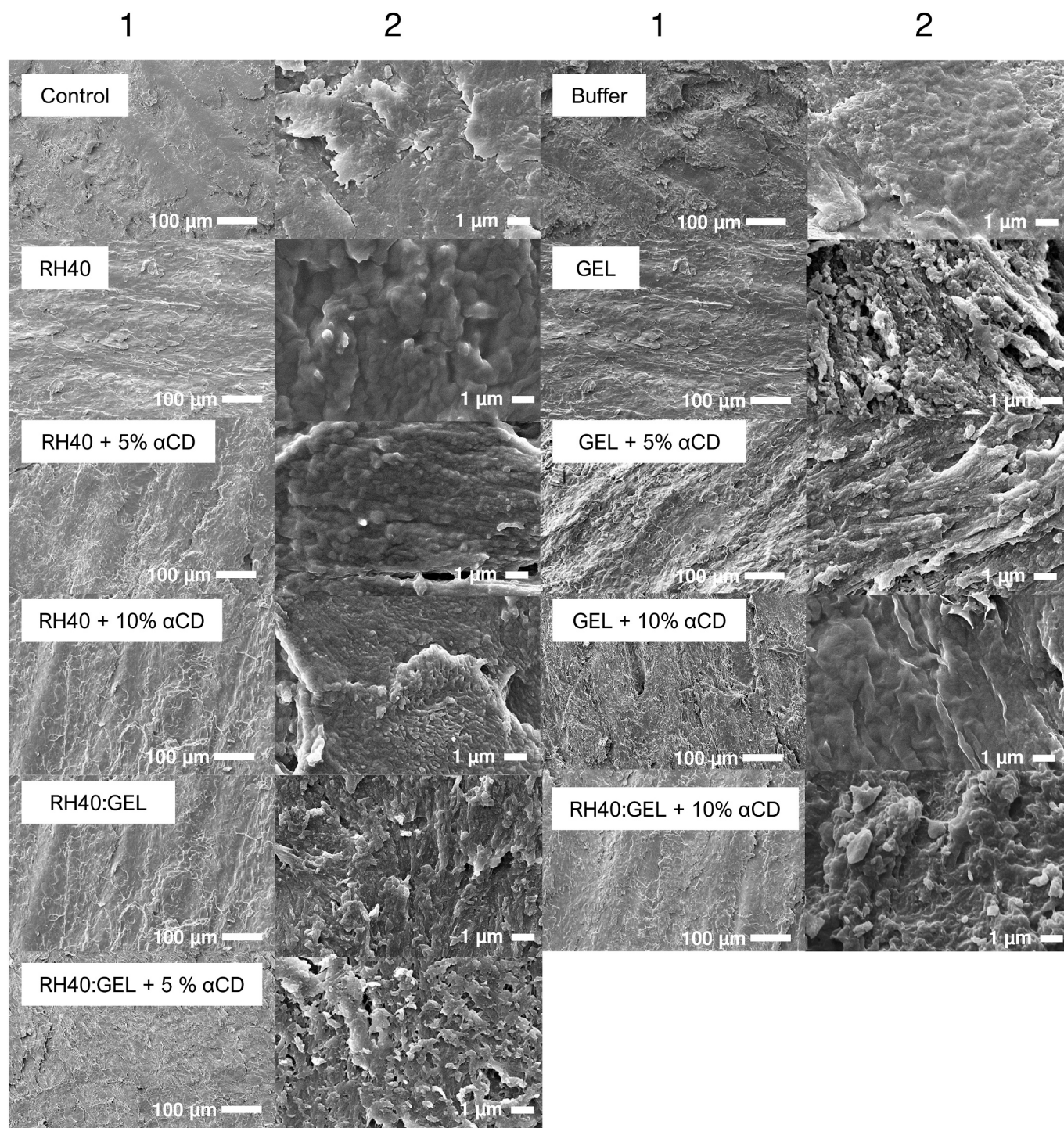CDs have already been studied as nail permeation enhancers

**Fig. 9.** SEM images of the surface of porcine hooves treated with the developed formulations at 200× (1) and 5000× (2) magnifications.

(Chouhan and Saini, 2014; Cutrin-Gomez et al., 2018c). However, αCD contribution to nail hydration has not been evaluated so far. In the tested concentrations, αCD provided considerably greater hydration than the control; HEF24 for αCD 5% and 10% was $1.24 \pm 0.01$ and $1.32 \pm 0.06$, respectively ($p < 0.05$). CDs have been described as capable of interacting with different proteins through amino acids, such as tyrosine, phenylalanine, and tryptophan residues in keratin. This interaction can lead to the loss of the protein structure by increasing the pores, swelling, and membrane flexibility (Cutrin-Gomez et al., 2018c).

We hypothesized that the association of surfactants and CDs would increase nail hydration. However, the formation of the supramolecular structured network affected the hydrating capability (Fig. 8). For instance, HEF24 values recorded for 5% αCD combined with GEL were similar to those of the control ($p > 0.05$) and significantly lower than observed with GEL solely ($p < 0.05$). In this case, the addition of αCD was not enough to increase hydration and, at the same time, compromised GEL interaction with the nail membrane. Differently, 10% αCD promoted the hydration capability of all formulations ($p < 0.05$) (Fig. 8). In PPR, αCD units are threaded in PEG units forming hydrogen bonds between neighboring αCDs. Thus, αCD is trapped in the three-dimensional network and less available to interact with the hooves' membrane. Probably, at the 10% concentration, αCD molecules may be

**Table 3**

Amount of TB released after 24 h, flux (*J*), and kinetics from surfactant dispersions and poly(pseudo)rotaxanes (PPR). Symbols indicate $p < 0.05$.

| Formulations | Amount of TB diffused ($\mu g/cm^2$) | $J$ ($\mu g/cm^2/$h) | Kinetics | $r^a$ |
|---|---|---|---|---|
| RH40 | $1150.50 \pm 35.83$ * | $51.87 \pm 7.63$ [#] | Zero Order | 0.9902 |
| GEL | $965.72 \pm 25.18$ | $40.35 \pm 0.61$ | Zero Order | 0.9771 |
| RH40:GEL | $1158.67 \pm 44.71$ * | $53.41 \pm 0.71$ [#] | Zero Order | 0.9829 |
| RH40 + 5% αCD | $741.13 \pm 46.84$ | $32.90 \pm 4.44$ | Higuchi | 0.9799 |
| GEL +5% αCD | $886.44 \pm 13.81$ | $34.26 \pm 1.63$ | Higuchi | 0.9854 |
| RH40:GEL +5% αCD | $813.78 \pm 35.13$ | $34.31 \pm 2.24$ | Zero Order | 0.9806 |
| RH40 + 10% αCD | $739.97 \pm 23.67$ | $30.70 \pm 5.54$ | Higuchi | 0.9734 |
| GEL +10% αCD | $732.59 \pm 50.74$ | $30.28 \pm 4.24$ | Higuchi | 0.9898 |
| RH40:GEL +10% αCD | $938.11 \pm 26.00$ ** | $33.68 \pm 5.06$ | Higuchi | 0.9864 |

[a] Linear correlation coefficient of 10 h experiment.

in excess and therefore free to interact with the hooves, providing greater hydration than formulations with 5% αCD.

Therefore, considering these results, formulations with 10% αCD could be pointed out as the most adequate since they combined sufficient viscosity for topical application and favored nail plate hydration, which in turn may be advantageous for drug permeation.

*3.7.2. Hooves microstructure*

The hydration effect was also observed by superficial alteration in the hooves through SEM (Fig. 9). Hooves without treatment (control) showed dense and compact structure, with the cells' edges overlapping (200× magnification), ensuring the nail barrier properties (Murdan, 2014). After 24 h in contact with citrate buffer, hooves absorbed water and increased 28% in their weight. No relevant changes in the surface of the citrate-swollen hooves were observed, even at the highest magnification (5000×), which reflected the inability of the buffer solution to modify ungual property.

Hooves exposed to micelles and PPR formulations evidenced remarkable changes in their surface. Numerous pores appeared in the

quite irregular structures. PPR formulations induced changes in hooves surface similar to those triggered by αCD solutions (Fig. S2, Supplementary Material). The interaction of αCD with the proteins and amino acids on the surface of hooves undoubtedly made possible the opening of these structures, increasing the expansion, and swelling of the nail plate, which led to the formation and increase of pores. Furthermore, more disorganized structure and larger pores were observed when 10% αCD solution and PPR formulations were applied, corroborating the results of the hydration study.

*3.8. In vitro drug release*

The developed formulations showed a variety of TB release profiles depending on the presence or absence of αCD (Fig. S3). RH40 and RH40:GEL micelles sustained TB release for 24 h, but the diffusion was faster than from GEL micelles ($p < 0.05$) (Table 3). This difference may be related to the higher G' and G" values of GEL micelles dispersions, which may hinder drug movement. Although mixed micelles were obtained combining both surfactants at the same amount, RH40 dictated the behavior of RH40:GEL micelles (Fig. S3, Supplementary Material).

The addition of αCD to the surfactant dispersions and consequent PPR formation led to a decrease in TB release. The more structured network due to PEG and αCD interaction may represent an additional obstacle for the drug to diffuse trough, as indicated by lower flux values (J) ($p < 0.05$).

Although the addition of increasing concentrations of αCD to the surfactant dispersions caused a notable difference in rheological behavior, i.e. 10% αCD led to stronger and more viscous PPR compared to 5% αCD, no differences were observed for TB release from RH40 + 5% and 10% αCD ($p > 0.05$). Thus, the increase in macroviscosity might not directly translate to microviscosity (Lorenzo-Veiga et al., 2019). This phenomenon could also be observed in GEL formulation. Despite the notable gain in viscosity, GEL +5% αCD released TB at the same rate as GEL micelles ($p > 0.05$).

Surprisingly, the formulation RH40: GEL +10% αCD did not cause further delay in TB release. The RH40 + GEL association can probably modify the interaction of surfactants with αCD, resulting in a higher fraction of free αCD, significantly impacting TB release.

*3.9. In vitro permeation studies*

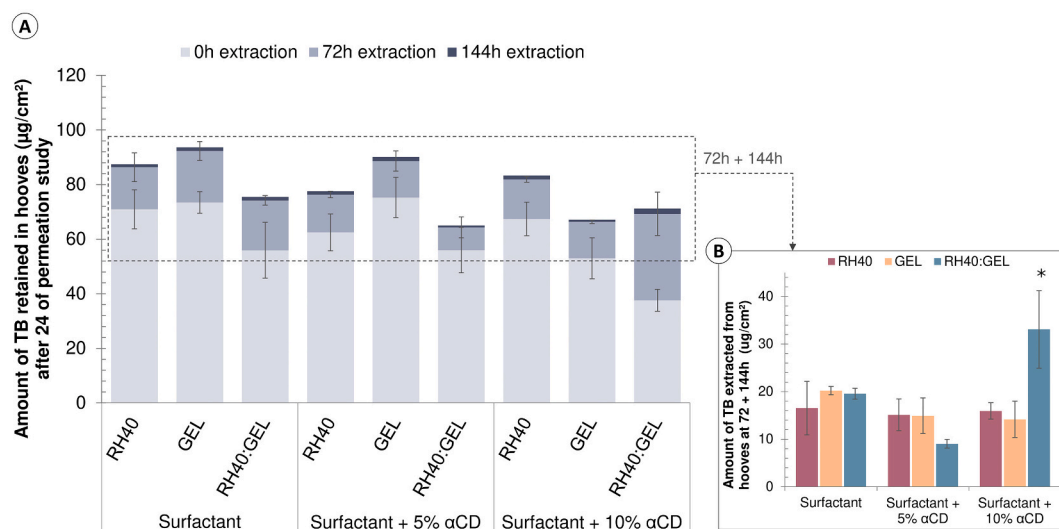The permeation studies revealed that after 24 h of contact of hooves

**Fig. 10.** TB retention in hooves ($\mu g/cm^2$) after topical application of different formulations (RH40, GEL, RH40: GEL with or without 5 or 10% αCD) for 24 h: a) Total amount of TB extracted immediately after the study (0 h extraction), 72 h after the study (72 h extraction) and 144 h after the study (144 h extraction) and b) Amount of TB extract in the second and third extraction procedure (72 + 144 h). *Symbols indicate statistically significant differences ($p < 0.05$).

with the formulations no drug was transferred to the receptor chamber. Hooves went through the extraction/depletion procedure to determine the amount of TB retained in the structure (Fig. 10). According to Rocha et al. (2017) and Krawczyk-Santos et al. (2021), the more time-consuming the extraction procedure indicates that the drug has penetrated deeper into the nail structure. Physical and chemical bonds present in nail keratin are responsible for its structural stability and hinder the permeation of molecules as a safety mechanism. Therefore, these bonds also make it difficult to extract the drug from the nail membrane (Murdan, 2002; Wang et al., 2016). Accordingly, it is essential to highlight that the drug accumulated in the nail plate can act as a reservoir, releasing the drug slowly to the surrounding tissues (Chen et al., 2021; Nair et al., 2009b; Nair et al., 2009c; Tanriverdi et al., 2016).

Considering the drug distribution in the different regions and layers of the nail plate, the amount of TB retained most superficially in hooves, indicated by the 0 h extraction results (Fig. 10a - light gray bars), was similar for all formulations, except for RH40: GEL +10% αCD, which presented a significantly reduced value ($p < 0.05$). Due to the reservoir feature of the nail plate previously mentioned, the amount of TB that penetrated more on the membrane surface could, over time, be distributed more deeply in a concentration gradient and even reach adjacent tissues such as nail bed and nail folds, which is possible due to the capacity of vertical and lateral diffusion in the nail plate. Such favorable penetration might reduce drug administration frequency and onychomycosis recurrence (Gratieri et al., 2017; Nair et al., 2010; Palliyil et al., 2014). The subsequent stages of the extraction by depletion (72 h and 144 h extraction) showed that TB was able to penetrate deeper regions of the nail plate and revealed that even though the drug has an excellent affinity for keratin (Matsuda et al., 2016), the developed formulations were able to promote favorable conditions for TB permeation into the membrane.

Although RH40: GEL +10% αCD caused lower accumulation of TB in the most external layers, a higher amount of TB was quantified after 72 and 144 h (Fig. 10b), which indicated TB penetration in the innermost regions of the hooves (Krawczyk-Santos et al., 2021; Rocha et al., 2017). The amount of drug extracted (72 and 144 h) was about two times greater for RH40: GEL +10% αCD compared to all other formulations (p < 0.05). Thus, probably the enhanced hydration of the nail membrane promoted by adding 10% αCD significantly improved TB permeation. Also, RH40: GEL +10% αCD may have higher concentration of free αCD, favoring TB release and directly contributing to drug permeation, as opposed to RH40: GEL +5% αCD (less free αCD and less TB diffused).

Another important benefit of this formulation is the gain in viscosity, which could prolong the time of permanence of the formulation at the application site. Moreover, the amount of TB retained in the hooves' membrane may be sufficient to exert its therapeutic effect. For instance, minimum inhibitory concentration (MIC) values reported for dermatophyte fungi vary from 0.3 to 1.0 µg/mL (Chouhan and Saini, 2014; Wiederhold et al., 2014), and RH40: GEL +10% αCD formulation delivered a mass amount about 230 times higher than the reported MIC.

## 4. Conclusion

Small amphiphilic surfactants RH40 and GEL and their mixture provided micelles with excellent capability to solubilize TB. Both surfactants interacted with αCD forming PPR, and drug solubilization was not detrimentally affected by the supramolecular structure formation. Also, changes in rheological properties were observed once PPR was formed. A remarkable increase in both G' and G" was noted, providing a significant increase in viscosity reflected in a slower drug release rate. Moreover, diluted formulations proved to be safe in contact with blood. The hydration study showed the potential of αCD, GEL micelles, and PPR with 10% αCD to interact with the hooves membrane, increasing pores and promoting the expansion of the structure, as confirmed by SEM images. This effect greatly impacted TB permeation, which was more

remarkable for RH40:GEL +10% αCD being able to deliver TB in considerable amounts to deeper regions of hooves. Overall, the results evidence the potential of using small surfactant micelles and PPR as water-based formulations for the topical treatment of onychomycosis. These systems have efficient solubilization properties, the surfactant can be used at high concentration without excessive increase in viscosity, and once the PPR is formed it can remain in the application site due to the enhanced viscoelastic properties. Moreover, micelles and PPR of RH40 and GEL could deliver TB in deeper regions of hooves in concentrations higher than MIC for dermatophytes, making them effective for topical treatment of onychomycosis.

## CRediT authorship contribution statement

**Anna Paula Krawczyk-Santos:** Data curation, Writing – original draft. **Ricardo Neves Marreto:** Writing – original draft. **Angel Concheiro:** Writing – review & editing. **Carmen Alvarez-Lorenzo:** Conceptualization, Supervision, Writing – review & editing. **Stephânia Fleury Taveira:** Conceptualization, Supervision, Writing – review & editing.

## Declaration of Competing Interest

The authors declare that they have no known competing financial interests or personal relationships that could have appeared to influence the work reported in this paper.

## Appendix A. Supplementary data

Supplementary data to this article can be found online at https://doi.org/10.1016/j.ijpx.2022.100118.

## References

AbdelSamie, S.M., Kamel, A.O., Sammour, O.A., Ibrahim, S.M., 2016. Terbinafine hydrochloride nanovesicular gel: in vitro characterization, ex vivo permeation and clinical investigation. Eur. J. Pharm. Sci. 88, 91–100. https://doi.org/10.1016/j.ejps.2016.04.004.

Albarahmieh, E., AbuAmmouneh, L., Kaddoura, Z., AbuHantash, F., Alkhalidi, B.A., Al-Halhouli, A., 2019. Fabrication of dissolvable microneedle patches using an innovative laser-cut mould design to shortlist potentially transungual delivery systems: in vitro evaluation. AAPS PharmSciTech 20, 1–14. https://doi.org/10.1208/s12249-019-1429-5.

Amin, K., Dannenfelser, R.-M., 2006. In vitro hemolysis: Guidance for the pharmaceutical scientist. J. Pharm. Sci. 95, 1173–1176. https://doi.org/10.1002/jps.20627.

Arenas, R., Torres-Guerrero, E., 2019. Chapter 4 - Onychomycosis. In: Tosti, A. (Ed.), Nail Disorders. Elsevier, pp. 31–35.

BASF, 2011. Technical Information - Kolliphor™ RH 40, pp. 1–8.

Baswan, S.M., Li, S.K., LaCount, T.D., Kasting, G.B., 2016. Size and charge dependence of ion transport in human nail plate. J. Pharm. Sci. 105, 1201–1208. https://doi.org/10.1016/j.xphs.2015.12.011.

BRASIL, 2017. Agência Nacional de Vigilância Sanitária. Resolução da Diretoria Colegiada - RDC N° 166, 24/07/2017 (Guia para validação de métodos analíticos).

Casiraghi, A., Selmin, F., Minghetti, P., Cilurzo, F., Montanari, L., 2015. Nonionic Surfactants: polyethylene glycol (PEG) ethers and fatty acid esters as penetration enhancers. In: Dragicevic, N., Maibach, H. (Eds.), Percutaneous Penetration Enhancers Chemical Methods in Penetration Enhancement. Springer, Berlin, Heidelberg. https://doi.org/10.1007/978-3-662-47039-8_15.

Chen, K., Puri, V., Michniak-Kohn, B., 2021. Iontophoresis to overcome the challenge of nail permeation: considerations and optimizations for successful ungual drug delivery. AAPS J. 23, 1–15. https://doi.org/10.1208/s12248-020-00552-y.

Chouhan, P., Saini, T.R., 2012. Hydration of nail plate: a novel screening model for transungual drug permeation enhancers. Int. J. Pharm. 436, 179–182. https://doi.org/10.1016/j.ijpharm.2012.06.020.

Chouhan, P., Saini, T.R., 2014. Hydroxypropyl-beta-cyclodextrin: a novel transungual permeation enhancer for development of topical drug delivery system for onychomycosis. J. Drug Deliv. 2014, 1–7. https://doi.org/10.1155/2014/950358.

Coleman, N.W., Fleckman, P., Huang, J.I., 2014. Fungal nail infections. J. Hand. Surg. [Am.] 39, 985–988. https://doi.org/10.1016/j.jhsa.2013.11.017.

Cutrin-Gomez, E., Anguiano-Igea, S., Delgado-Charro, M.B., Gomez-Amoza, J.L., Otero-Espinar, F.J., 2018a. Effect of penetration enhancers on drug nail permeability from cyclodextrin/poloxamer-soluble polypseudorotaxane-based nail lacquers. Pharmaceutics 10, 1–18. https://doi.org/10.3390/pharmaceutics10040273.

Cutrin-Gomez, E., Anguiano-Igea, S., Delgado-Charro, M.B., Gomez-Amoza, J.L., Otero-Espinar, F.J., 2018b. Effect on nail structure and transungual permeability of the ethanol and poloxamer ratio from cyclodextrin-soluble polypseudorotaxanes based nail lacquer. Pharmaceutics 10, 1–15. https://doi.org/10.3390/pharmaceutics10030156.

Cutrin-Gomez, E., Anguiano Igea, S., Gomez Amoza, J.L., Otero Espinar, F.J., 2018c. Evaluation of the promoting effect of soluble cyclodextrins in drug nail penetration. Eur. J. Pharm. Sci. 117, 270–278. https://doi.org/10.1016/j.ejps.2018.02.028.

Darkes, M.J.M., Scott, L.J., Goa, K.L., 2003. Terbinafine. Am. J. Clin. Dermatol. 4, 39–65. https://doi.org/10.2165/00128071-200304010-00005.

Elsayed, M.M., 2015. Development of topical therapeutics for management of onychomycosis and other nail disorders: a pharmaceutical perspective. J. Control. Release 199, 132–144. https://doi.org/10.1016/j.jconrel.2014.11.017.

Elsherif, N.I., Shamma, R.N., Abdelbary, G., 2017. Terbinafine hydrochloride trans-ungual delivery via nanovesicular systems: in vitro characterization and ex vivo evaluation. AAPS PharmSciTech 18, 551–562. https://doi.org/10.1208/s12249-016-0528-9.

EMA, European Medicines Agency, 2014. Background Review for Cyclodextrins Used as Excipients. https://www.ema.europa.eu/en/documents/report/background-review-cyclodextrins-used-excipients-context-revision-guideline-excipients-label-package_en.pdf.

Gattéfossé, 2018. Gelucire® 48/16 Pellets - Solubility and Oral Bioavailability Enhancement, pp. 1–16.

Ghannoum, M.A., Long, L., Pfister, W.R., 2009. Determination of the efficacy of terbinafine hydrochloride nail solution in the topical treatment of dermatophytosis in a guinea pig model. Mycoses 52, 35–43. https://doi.org/10.1111/j.1439-0507.2008.01540.x.

Ghannoum, M., Long, L., Kunze, G., Sarkany, M., Osman-Ponchet, H., 2019. A pilot, layerwise, ex vivo evaluation of the antifungal efficacy of amorolfine 5% nail lacquer vs other topical antifungal nail formulations in healthy toenails. Mycoses 62, 494–501. https://doi.org/10.1111/myc.12896.

Gratieri, T., Krawczyk-Santos, A.P., da Rocha, P.B.R., Cunha-Filho, M., Gelfuso, G.M., Marreto, R.N., Taveira, S.F., 2017. SLN- and NLC-encapsulating antifungal agents: skin drug delivery and their unexplored potential for treating onychomycosis. Curr. Pharm. Des. 23, 1–12. https://doi.org/10.2174/1381612823666171115112745.

Gregori Valdes, B.S., Serro, A.P., Gordo, P.M., Silva, A., Goncalves, L., Salgado, A., Marto, J., Baltazar, D., Dos Santos, R.G., Bordado, J.M., Ribeiro, H.M., 2017. New polyurethane nail lacquers for the delivery of terbinafine: formulation and antifungal activity evaluation. J. Pharm. Sci. 106, 1570–1577. https://doi.org/10.1016/j.xphs.2017.02.017.

Gunt, H.B., Miller, M.A., Kasting, G.B., 2007. Water diffusivity in human nail plate. J. Pharm. Sci. 96, 3352–3362. https://doi.org/10.1002/jps.20988.

Hussein, Y.H.A., Youssry, M., 2018. Polymeric micelles of biodegradable diblock copolymers: enhanced encapsulation of hydrophobic drugs. Materials (Basel) 11, 1–26. https://doi.org/10.3390/ma11050688.

Kerai, L.V., Bardes, J., Hilton, S., Murdan, S., 2018. Two strategies to enhance ungual drug permeation from UV-cured films: Incomplete polymerisation to increase drug release and incorporation of chemical enhancers. Eur. J. Pharm. Sci. 123, 217–227. https://doi.org/10.1016/j.ejps.2018.07.049.

Krawczyk-Santos, A.P., da Rocha, P.B.R., Kloppel, L.L., Souza, B.D.S., Anjos, J.L.V., Alonso, A., de Faria, D.L.A., Gil, O.M., Gratieri, T., Marreto, R.N., Taveira, S.F., 2021. Enhanced nail delivery of voriconazole-loaded nanomicelles by thioglycolic acid pretreatment: a study of protein dynamics and disulfide bond rupture. Int. J. Pharm. 602, 1–12. https://doi.org/10.1016/j.ijpharm.2021.120597.

Lorenzo-Veiga, B., Sigurdsson, H.H., Loftsson, T., Alvarez-Lorenzo, C., 2019. Cyclodextrin-amphiphilic copolymer supramolecular assemblies for the ocular delivery of natamycin. Nanomaterials 9, 1–18. https://doi.org/10.3390/nano9050745.

Lusiana, Muller-Goymann, C.C., 2011. Preparation, characterization, and in vitro permeation study of terbinafine HCl in poloxamer 407-based thermogelling formulation for topical application. AAPS PharmSciTech 12, 496–506. https://doi.org/10.1208/s12249-011-9611-4.

Manjappa, A.S., Kumbhar, P.S., Patil, A.B., Disouza, J.I., Patravale, V.B., 2019. Polymeric mixed micelles: improving the anticancer efficacy of single-copolymer micelles. Crit. Rev. Ther. Drug Carrier Syst. 36, 1–58. https://doi.org/10.1615/CritRevTherDrugCarrierSyst.2018020481.

Marcos, X., Perez-Casas, S., Llovo, J., Concheiro, A., Alvarez-Lorenzo, C., 2016. Poloxamer-hydroxyethyl cellulose-alpha-cyclodextrin supramolecular gels for sustained release of griseofulvin. Int. J. Pharm. 500, 11–19. https://doi.org/10.1016/j.ijpharm.2016.01.015.

Marreto, R.N., Cardoso, G., Dos Santos Souza, B., Martin-Pastor, M., Cunha-Filho, M., Taveira, S.F., Concheiro, A., Alvarez-Lorenzo, C., 2020. Hot melt-extrusion improves the properties of cyclodextrin-based poly(pseudo)rotaxanes for transdermal formulation. Int. J. Pharm. 586, 119510 https://doi.org/10.1016/j.ijpharm.2020.119510.

Matsuda, Y., Sugiura, K., Hashimoto, T., Ueda, A., Konno, Y., Tatsumi, Y., 2016. Efficacy coefficients determined using nail permeability and antifungal activity in keratin-containing media are useful for predicting clinical efficacies of topical drugs for onychomycosis. PLoS One 11, 1–12. https://doi.org/10.1371/journal.pone.0159661.

Motoyama, K., Arima, H., Toyodome, H., Irie, T., Hirayama, F., Uekama, K., 2006. Effect of 2,6-di-O-methyl-α-cyclodextrin on hemolysis and morphological change in rabbit's red blood cells. Eur. J. Pharm. Sci. 29, 111–119. https://doi.org/10.1016/j.ejps.2006.06.002.

Murdan, S., 2002. Drug delivery to the nail following topical application. Int. J. Pharm. 236, 1–26. https://doi.org/10.1016/s0378-5173(01)00989-9.

Murdan, S., 2014. Focal drug delivery to the nail. In: Domb, A.J., Khan, W. (Eds.), Focal Controlled Drug Delivery. Springer US, Boston, MA, pp. 561–584.

Nair, A.B., Kim, H.D., Chakraborty, B., Singh, J., Zaman, M., Gupta, A., Friden, P.M., Murthy, S.N., 2009a. Ungual and trans-ungual iontophoretic delivery of terbinafine for the treatment of onychomycosis. J. Pharm. Sci. 98, 4130–4140. https://doi.org/10.1002/jps.21711.

Nair, A.B., Sammeta, S.M., Kim, H.D., Chakraborty, B., Friden, P.M., Murthy, S.N., 2009b. Alteration of the diffusional barrier property of the nail leads to greater terbinafine drug loading and permeation. Int. J. Pharm. 375, 22–27. https://doi.org/10.1016/j.ijpharm.2009.03.012.

Nair, A.B., Vaka, S.R., Sammeta, S.M., Kim, H.D., Friden, P.M., Chakraborty, B., Murthy, S.N., 2009c. Trans-ungual iontophoretic delivery of terbinafine. J. Pharm. Sci. 98, 1788–1796. https://doi.org/10.1002/jps.21555.

Nair, A.B., Chakraborty, B., Murthy, S.N., 2010. Effect of polyethylene glycols on the trans-ungual delivery of terbinafine. Curr. Drug Deliv. 7, 407–414. https://doi.org/10.2174/156720110793566308.

Naumann, S., Meyer, J.P., Kiesow, A., Mrestani, Y., Wohlrab, J., Neubert, R.H., 2014. Controlled nail delivery of a novel lipophilic antifungal agent using various modern drug carrier systems as well as in vitro and ex vivo model systems. J. Control. Release 180, 60–70. https://doi.org/10.1016/j.jconrel.2014.02.013.

Nogueiras-Nieto, L., Gomez-Amoza, J.L., Delgado-Charro, M.B., Otero-Espinar, F.J., 2011. Hydration and N-acetyl-l-cysteine alter the microstructure of human nail and bovine hoof: implications for drug delivery. J. Control. Release 156, 337–344. https://doi.org/10.1016/j.jconrel.2011.08.021.

Nogueiras-Nieto, L., Begona Delgado-Charro, M., Otero-Espinar, F.J., 2013. Thermogelling hydrogels of cyclodextrin/poloxamer polypseudorotaxanes as aqueous-based nail lacquers: application to the delivery of triamcinolone acetonide and ciclopirox olamine. Eur. J. Pharm. Biopharm. 83, 370–377. https://doi.org/10.1016/j.ejpb.2012.11.004.

Ogino, K., Onoe, Y., Abe, M., Ono, H., Bessho, K., 1990. Reduction of surface tension by novel polymer surfactants. Langmuir 6, 1330. https://doi.org/10.1021/la00097a025.

Palliyil, B.B., Li, C., Owaisat, S., Lebo, D.B., 2014. Lateral drug diffusion in human nails. AAPS PharmSciTech 15, 1429–1438. https://doi.org/10.1208/s12249-014-0169-9.

Patel, M.M., Vora, Z.M., 2016. Formulation development and optimization of transungual drug delivery system of terbinafine hydrochloride for the treatment of onychomycosis. Drug Deliv. Transl. Res. 6, 263–275. https://doi.org/10.1007/s13346-016-0287-x.

Repka, M.A., O'Haver, J., See, C.H., Gutta, K., Munjal, M., 2002. Nail morphology studies as assessments for onychomycosis treatment modalities. Int. J. Pharm. 245, 25–36. https://doi.org/10.1016/s0378-5173(02)00321-6.

Rocha, K.A.D., Krawczyk-Santos, A.P., Andrade, L.M., Souza, L.C.D., Marreto, R.N., Gratieri, T., Taveira, S.F., 2017. Voriconazole-loaded nanostructured lipid carriers (NLC) for drug delivery in deeper regions of the nail plate. Int. J. Pharm. 531, 292–298. https://doi.org/10.1016/j.ijpharm.2017.08.115.

Sachdeva, V., Kim, H.D., Friden, P.M., Banga, A.K., 2010. Iontophoresis mediated in vivo intradermal delivery of terbinafine hydrochloride. Int. J. Pharm. 393, 113–119. https://doi.org/10.1016/j.ijpharm.2010.04.014.

Shivakumar, H.N., Vaka, S.R., Madhav, N.V., Chandra, H., Murthy, S.N., 2010. Bilayered nail lacquer of terbinafine hydrochloride for treatment of onychomycosis. J. Pharm. Sci. 99, 4267–4276. https://doi.org/10.1002/jps.22150.

Simões, S.M., Rey-Rico, A., Concheiro, A., Alvarez-Lorenzo, C., 2015. Supramolecular cyclodextrin-based drug nanocarriers. Chem. Commun. 51, 6275–6289. https://doi.org/10.1039/c4cc10388b.

Sobczyński, J., Chudzik-Rząd, B., 2018. Mixed micelles as drug delivery nanocarriers. In: Grumezescu, A.M. (Ed.), Design and Development of New Nanocarriers. William Andrew Publishing, pp. 331–364. https://doi.org/10.1016/B978-0-12-813627-0.00009-0.

Szente, L., Puskás, I., Csabai, K., Fenyvesi, É., 2014. Supramolecular proteoglycan aggregate mimics: cyclodextrin-assisted biodegradable polymer assemblies for electrostatic-driven drug delivery. Chem. Asian J. 9, 1365–1372. https://doi.org/10.1002/asia.201301391.

Tanriverdi, S.T., Hilmioglu Polat, S., Yesim Metin, D., Kandiloglu, G., Ozer, O., 2016. Terbinafine hydrochloride loaded liposome film formulation for treatment of onychomycosis: in vitro and in vivo evaluation. J. Liposome Res. 26, 163–173. https://doi.org/10.3109/08982104.2015.1067892.

Taveira, S.F., Varela-Garcia, A., Dos Santos Souza, B., Marreto, R.N., Martin-Pastor, M., Concheiro, A., Alvarez-Lorenzo, C., 2018. Cyclodextrin-based poly(pseudo)rotaxanes for transdermal delivery of carvedilol. Carbohydr. Polym. 200, 278–288. https://doi.org/10.1016/j.carbpol.2018.08.017.

Thatai, P., Sapra, B., 2017. Transungual gel of terbinafine hydrochloride for the management of onychomycosis: formulation, optimization, and evaluation. AAPS PharmSciTech 18, 2316–2328. https://doi.org/10.1208/s12249-017-0711-7.

Thatai, P., Sapra, B., 2018. Terbinafine hydrochloride nail lacquer for the management of onychomycosis: formulation, characterization and in vitro evaluation. Ther. Deliv. 9, 99–119. https://doi.org/10.4155/tde-2017-0069.

Uzqueda, M., Martín, C., Zornoza, A., Sánchez, M., Vélaz, I., 2009. Physicochemical characterization of terbinafine-cyclodextrin complexes in solution and in the solid state. J. Incl. Phenom. Macrocycl. Chem. 66, 393–402. https://doi.org/10.1007/s10847-009-9656-0.

Uzqueda, M., Martín, C., Zornoza, A., Sánchez, M., Vélaz, I., 2010. Physicochemical characterization of terbinafine-cyclodextrin complexes in solution and in the solid state. J. Incl. Phenom. Macrocycl. Chem. 66, 393–402. https://doi.org/10.1007/s10847-009-9656-0.

Vejnovic, I., Huonder, C., Betz, G., 2010a. Permeation studies of novel terbinafine formulations containing hydrophobins through human nails in vitro. Int. J. Pharm. 397, 67–76. https://doi.org/10.1016/j.ijpharm.2010.06.051.

Vejnovic, I., Simmler, L., Betz, G., 2010b. Investigation of different formulations for drug delivery through the nail plate. Int. J. Pharm. 386, 185–194. https://doi.org/10.1016/j.ijpharm.2009.11.019.

Wang, B., Yang, W., McKittrick, J., Meyers, M.A., 2016. Keratin: Structure, mechanical properties, occurrence in biological organisms, and efforts at bioinspiration. Prog. Mater. Sci. 76, 229–318. https://doi.org/10.1016/j.pmatsci.2015.06.001.

Wiederhold, N.P., Fothergill, A.W., McCarthy, D.I., Tavakkol, A., 2014. Luliconazole demonstrates potent in vitro activity against dermatophytes recovered from patients with onychomycosis. Antimicrob. Agents Chemother. 58, 3553–3555. https://doi.org/10.1128/AAC.02706-13.

Zhou, T., Zhu, L., Xia, H., He, J., Liu, S., He, S., Wang, L., Zhang, J., 2017. Micelle carriers based on macrogol 15 hydroxystearate for ocular delivery of terbinafine hydrochloride: in vitro characterization and in vivo permeation. Eur. J. Pharm. Sci. 109, 288–296. https://doi.org/10.1016/j.ejps.2017.08.020.